IOP Conf. Series: Materials Science and Engineering **377** (2018) 012203 doi:10.1088/1757-899X/377/1/012203

RSM Based Experimental Investigation and Analysis into Laser Surface Texturing on Titanium using Pulsed Nd:YAG Laser

G. Kibria[1], S. Chatterjee[2], I. Shivakoti[2], B. Doloi[3], B. Bhattacharyya[3]

[1]Department of Mechanical Engineering, Aliah University, Kolkata-700156, India
[2]Department of Mechanical Engineering, Sikkim Manipal Institute of Technology, Sikkim Majitar, Rangpo, Sikkim 737132, India
[3]Production Engineering Department, Jadavpur University, Kolkata-700032, India

Corresponding author's e-mail address: saikatchatterjee007@gmail.com

Abstract. Recently, production of defined surfaces with required tribological properties in different biomedical materials is in high demand. Amongst various non-traditional machining processes, laser surface texturing is a novel machining technique by which this type of tribological surfaces can be generated efficiently and effectively. In the present paper, an attempt has been made to carry out experimentation and analysis in laser surface texturing process on commercially available pure titanium material employing a pulsed Nd:YAG laser system. Response surface methodology (RSM) based design of experiments was implemented to conduct the experiments and further analysis of results obtained. Utilizing four process variables, each has five levels, experiments were conducted based on laser scanning methodology and surface roughness (Ra and Rz) were measured. Empirical models were also developed for establishing relationships between process parameters and performance criteria. Multi-objective optimization was conducted to achieve minimum value of surface roughness and contact angle.

1. Introduction

Laser micro-machining is the process which deals with manufacture of micro profile or surface on advanced engineering materials using highly focused intense laser beam. Recently, the use of laser has tremendously increased to process difficult-to-cut materials especially engineering ceramics. This is due to certain advantages of laser beam over other cutting tools. These are, one-step direct and locally confined machining, no induced mechanical stresses on machined surface, green and clean technology, elimination of secondary operations, less material wastage as chips and less cycle time [1,2]. Furthermore, with significant development of material science research, various engineering materials including high strength and temperature resisting (HSTR) materials are being developed in recent times for successfully implementing in product manufacturing and further effective utilization [3, 4]. Since last two decades, laser beam micromachining processes are being utilized for micromachining of advanced engineering materials to meet the requirements of industries like micro-reactors, electronics, bio-medical, chemical and sensors-actuators [5, 6].

Already, several laser micromachining processes such as micro-drilling, micro-cutting, micro-turning, micro-channeling, surface modification, micro-grooving etc have successfully implemented in manufacturing of macro and micro products with specific surface features and geometrical dimensions. Laser surface texturing is a novel micromachining technique in which defined featured surface can be generated on advanced engineering materials for enhancing the tribological properties of mating parts of the components [7-9]. This novel surface machining process can significantly improve several aspects such as wetting characteristics, load capabilities, wear resistance and lubrication. In this process, a focused laser beam is irradiated onto the surface of workpiece in such a defined pattern by controlling X Y table movement so that laser textured surface with defined surface characteristics is generated. Thus, laser beam scanning is carried out on the surface with overlaps between two consecutive laser scan tracks. The amount of this overlap is controlled by the value of transverse feed. With more number of laser scan passes, one can generate specific depth of laser surface texture with defined surface features. The schematic of laser beam scan pattern is viewed in Figure 1. The schematic representation of these two overlaps with laser scanning direction is depicted in Figure 2. On the other hand, Titanium is an attractive material for numerous industries such as aerospace, biomedical, sports, architecture etc for its diversified properties such as extremely tough, lightweight, high strength to weight ratio, corrosion resistance, biological compatibility, low density, low coefficient of thermal expansion and stability at elevated temperature. Pure titanium is one of the biologically inert biomaterials as it exhibits property of high biocompatibility with tissue and blood. Due to this, this material is largely used for fabricating biomedical implants.

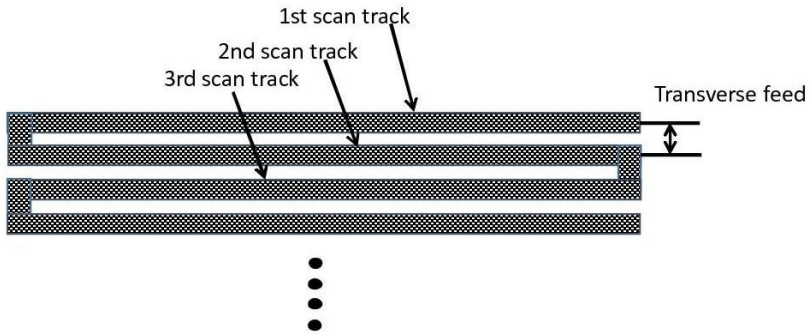

Figure 1. Schematic of laser beam scan pattern during laser surface texturing process

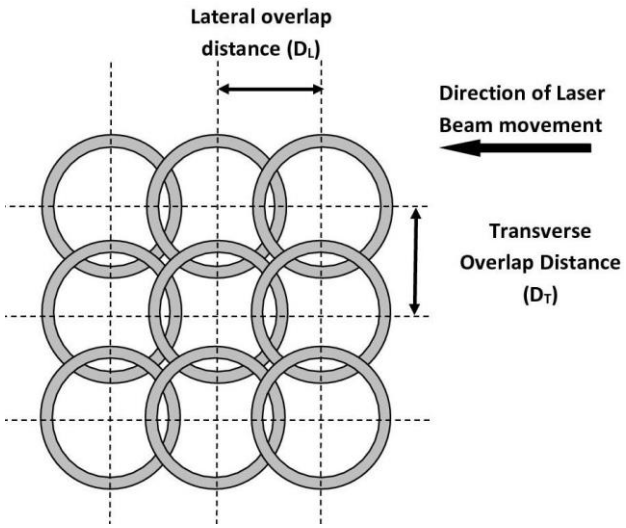

Figure 2. Scheme of laser scanning strategy showing the lateral and transverse overlap distance

In the literature, limited research work has been performed by various researchers and academia in the area of laser surface texturing on different engineering materials using various types of laser. Cunha et al. [7] carried out research on surface texturing using direct laser writing methods and ultrashort laser pulses on titanium and Ti–6Al–4V alloy. Kovalchenko et al. [10] carried out tribological experiments on pin-on-disk test apparatus at sliding speeds of ranged from 0.15 to 0.75 m/s and nominal contact pressures of a range from 0.16 to 1.6 MPa. The authors found that the laser texturing expanded the range of speed-load parameters for hydrodynamic lubrication. Li et al. [11] demonstrated the fabrication of stable super-hydrophilic and super-hydrophobic textured titanium surface using femtosecond pulsed laser. Soveja et al. [12] investigated the influence of the operating factors on the laser texturing process using two experimental design approaches (Taguchi method and RSM method) on TA6V alloy. Tripathi et al. [13] studied the effect of laser surface texturing on friction and wear behavior of graphite cast iron. In this work, authors successfully produced dimples of dimension of diameter 60 μm and depth 30 μm with a dimple pitch of 80-200 μm. Velasquez et al. [14] studied the effect of surface texturing on the surgical blade by developing micro dimples of dimension 110 μm in diameter and 30 μm in depth on cutting edge surface of surgical blades by an 8 ps pulsed Nd:YVO4 laser. From the literature review, it was found that very few experimental research have been done to study the influencing process parameters on surface characteristics and the effect of overlap factors on surface conditions during laser surface texturing process. Furthermore, as the process involves a number of process parameters, the selection of suitable process parameter setting is very difficult task for achieving the desired surface characteristics. To meet the micro manufacturing demands and also to explore the influences of different process parameters on surface characteristics, in the present paper, attempts have been made to conduct experiments in laser surface texturing process on titanium material considering process parameters such as laser beam average power, pulse frequency, laser beam scanning speed and transverse feed.

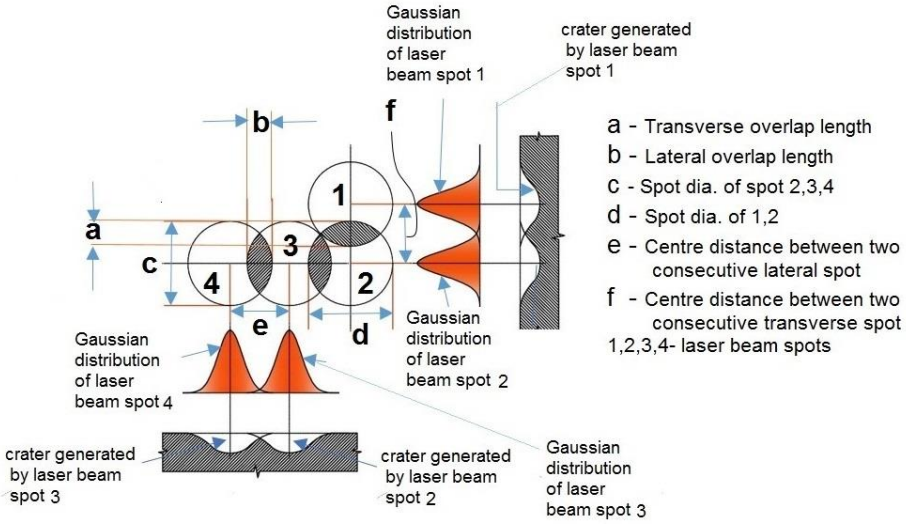

Figure 3. Schematic view of laser surface texturing scanning strategy showing lateral and transverse overlap and Gaussian energy distribution pattern for laser spots

In laser texturing process, two overlap factors, i.e. lateral overlap and transverse overlap are very important and major criteria for achieving qualitative and defined surface. Therefore, the basic understanding of lateral overlap and transverse overlap of laser beam scanning is very much needed. The schematic representation of laser beam scan pattern with two overlaps is viewed in Figure 3. The schematic representation also shows the Gaussian energy distributions of laser spots as well as the craters generated by these laser spots. The amount of lateral overlap and transverse overlap should be chosen very carefully as these overlaps depend upon the various parametric settings of process parameters. The mathematical relationship between various factors and the above-mentioned overlaps can be calculated as follows [15].

$$Transverse\ overlap\ (O_T) = \frac{D - D_T}{D} \times 100\% \quad (1)$$

$$Lateral\ overlap\ (O_L) = \frac{D - D_L}{D} \times 100\% \quad (2)$$

Here, D is the spot diameter of the laser beam at focused zone in mm, D_L (D_L=Vin/f) is lateral overlap distance in mm; Vin is the laser beam scanning speed in mm/s, f is pulse frequency in Hz, D_T is the transverse overlap distance in mm. According to equation (1), it is very clear that the lateral overlap area can be increased by either increasing the pulse frequency or by reducing the laser beam scanning speed. Equation (2) depicts the relation of transverse overlap area with transverse feed. It is theoretically very clear than the transverse overlap area, i.e., overlap of two consecutive laser spot in transverse direction, can be increased by decreasing the transverse feed or reducing the centre distance between two consecutive spots.

2. Experimental conditions and planning

All the experiments were conducted in CNC controlled pulsed Nd:YAG laser beam micromachining system of average power 50W (make: M/S Sahajanand Laser Technology Limited, Pune, India). In the present experimental investigation, the process parameters, which have been selected for conducting laser surface texturing process of pure titanium, are laser beam average power (4, 5.5, 7, 8.5 and 10W), pulse frequency (600, 800, 1000, 1200 and 1400 Hz), laser beam scanning speed (1, 2, 3, 4 and 5 mm/s) and transverse feed (0.01, 0.02, 0.03, 0.04 and 0.05 mm). Flat titanium work piece of dimension 50mm×50mm×1mm is considered in the experimentation. Response Surface Methodology (RSM) based design of experiments is utilized to for constructing the combinations of process parameters based on the selected vales of process parameters and number of levels. Four process parameters each parameter having four levels require a total of 31 number of experiments. Considering the ranges of process parameters taken in this research study, the values of lateral overlap and transverse overlap have been calculated using equations (1) and (2). The values of lateral overlap are more than 95%, which ensures that quality surface can be achieved by laser surface texturing process. The calculated values of transverse overlap are in the range of 50 to 90%. This wide range of overlap has been considered to study and analysis the effect of these overlaps on surface characteristics to be obtained. The other details and conditions of the machining setup aare depicted in Table 1. After conducting experiments, response criteria surface roughness (Ra and Rz) both in lateral and transverse directions using roughness measuring instruments, Mitutoyo Surftest SJ-210. During surface roughness measurement, the cut off length and total length of measurement were kept as 0.8 and 5mm respectively. The values of surface roughness along the laser scan line (lateral direction) is termed as surface roughness (Ra and Rz) in lateral direction whereas the values of surface roughness obtained along the perpendicular of lateral direction (i.e. transverse direction) is termed as surface roughness (Ra and Rz) in transverse direction. The results were analysed using various surface plots.

Table 1. Experimental conditions for laser surface texturing

Conditions	Description
Laser type	Nd:YAG Laser (pulsed)
Wavelength	1064 nm
Mode of operation	Q-switched (pulsed)
Mode of laser beam	Fundamental mode (TEM_{00})
Mirror reflectivity	Rear mirror 100% and front mirror 80%
Pulse width, % of duty cycle	Variable
Air pressure, kgf/cm^2	1.3
Z feed rate, mm/s	0.01

Table 2. RSM based design of experiments and results of responses

Exp. No.	Avg. Power (W)	Pulse Freq. (µm)	Scanning Speed (mm/s)	Transverse Feed (mm)	S. Roughness (L), Ra (µm)	S. Roughness (T), Ra (µm)	S. Roughness (L), Rz (µm)	S. Roughness (T), Rz (µm)
1	7.0	1000	3	0.03	11.75	6.91	61.06	37.49
2	8.5	1200	4	0.04	5.02	4.99	29.86	25.60
3	8.5	800	2	0.04	6.98	7.11	42.46	35.99
4	5.5	800	4	0.02	8.68	6.32	47.05	33.03
5	8.5	800	4	0.04	11.50	8.25	59.66	41.66
6	5.5	1200	2	0.02	3.68	3.62	21.54	20.11
7	8.5	800	2	0.02	13.66	9.91	72.54	48.15
8	8.5	1200	2	0.02	7.32	4.56	40.50	23.55
9	7.0	1000	3	0.03	12.70	7.73	65.42	38.95
10	5.5	1200	4	0.04	4.91	4.55	31.62	23.80
11	5.5	800	2	0.04	7.53	5.22	40.15	25.63
12	7.0	1000	1	0.03	6.07	4.86	36.60	29.20
13	10.0	1000	3	0.03	12.06	7.35	72.18	37.43
14	7.0	1000	3	0.05	9.84	7.41	53.13	34.30
15	8.5	1200	2	0.04	5.13	5.32	33.60	31.14
16	7.0	1000	3	0.01	10.23	7.57	53.91	35.80
17	7.0	1000	3	0.03	11.10	7.62	55.45	39.12
18	7.0	1000	3	0.03	10.25	8.62	60.59	40.54
19	5.5	1200	2	0.04	3.57	3.58	24.16	18.48
20	5.5	1200	4	0.02	6.25	5.32	40.50	27.22
21	7.0	1000	5	0.03	9.73	7.18	52.22	39.17
22	7.0	600	3	0.03	10.64	9.53	57.04	45.85
23	7.0	1000	3	0.03	11.93	8.18	68.73	42.35
24	4.0	1000	3	0.03	3.82	3.95	24.27	20.94
25	7.0	1000	3	0.03	13.86	9.65	74.94	46.47
26	8.5	800	4	0.02	12.88	7.07	72.90	39.37
27	7.0	1000	3	0.03	14.64	9.62	75.54	48.81
28	5.5	800	4	0.04	6.97	7.08	38.36	35.41
29	7.0	1400	3	0.03	5.70	5.82	32.43	28.82
30	8.5	1200	4	0.02	7.50	4.70	42.53	25.50
31	5.5	800	2	0.02	10.25	7.17	53.76	34.08

3. Results and Discussions

Using statistical analysis software and based on the results of response criteria i.e. surface roughness (Ra and Rz) achieved as shown in Table 2, mathematical models of responses have been developed for establishing the relationship between various process parameters and performance criteria. The details of developed mathematical models of responses are shown in equations (3) to (6).

$$Y_{RaL}=-59.44+10.35\times X_1+0.05\times X_2+5.83\times X_3+262.35\times X_4-0.55\times X_1^2-1.25\times X_3^2 -7203.72\times X_4^2+0.08\times X_1X_3-28.54\times X_1X_4+0.20\times X_2X_4+29.94\times X_3X_4 \quad (3)$$

$$Y_{RaT}=-24.08+6.79\times X_1+0.01\times X_2+4.13\times X_3-47.01\times X_4-0.36\times X_1^2-0.71\times X_3^2-3416.52\times X_4^2 -0.23\times X_1X_3+5.96\times X_1X_4+0.10\times X_2X_4+34.31\times X_3X_4 \quad (4)$$

$$Y_{RzL}=-313.5+50.4\times X_1+0.3\times X_2+34.4\times X_3+1604.7\times X_4-2.3\times X_1^2-6.1\times X_3^2-38642.1\times X_4^2 -0.1\times X_1X_3-143.0\times X_1X_4+1.2\times X_2X_4+28.1\times X_3X_4 \quad (5)$$

$$Y_{RzT}=-135.2+32.5\times X_1+0.1\times X_2+20.6\times X_3+166.8\times X_4-1.7\times X_1^2-2.5\times X_3^2-22934.8\times X_4^2 -1.2\times X_1X_3+37.2\times X_1X_4+0.6\times X_2X_4+100.0\times X_3X_4 \quad (6)$$

Here, X_1, X_2, X_3 and X_4 are the uncoded values of laser beam average power, pulse frequency, scanning speed and transverse feed, respectively. To validate these empirical equations, analysis of variance (ANOVA) test was performed and the calculated F values and p values are shown in Table 3. The standard F-value for lack-of-fit is 4.06 for 95% confidence level. However, the calculated F-values for surface roughness (lateral), surface roughness (transverse) and contact angle are 1.43, 0.97, 1.51, 1.11 and 1.66 respectively at 95% confidence level. These values are lower than the standard F-value. This implies that the developed empirical models are adequate at 95% confidence level and valid in the ranges of process parameters. The p-values of lack of fit for these five response criteria are 0.344, 0.542, 0.317, 0.471 and 0.276, indicating that the models adequately fit the data and ensure that the models can well correlate the responses. Moreover, to verify the adequacy of the developed models in the selected ranges of process parameters, eight verification experiments were performed and the results of responses were compared with RSM based model predicted data. It was observed that the average predicted error is 3.18% which is within the acceptable limit.

Table 3. Results of analysis of variance (ANOVA) test for responses

Source	DF	Surface Roughness (L), Ra		Surface Roughness (T), Ra		Surface Roughness (L), Rz		Surface Roughness (T), Rz	
		F value	p value	F value	p value	F value	p value	F value	p value
Regression	14	6.63	0.000	5.80	0.001	6.42	0.000	7.01	0.000
Linear	4	3.99	0.020	5.01	0.008	3.99	0.020	6.04	0.004
Square	4	9.33	0.000	7.49	0.001	8.45	0.001	8.50	0.001
Interaction	6	0.51	0.794	0.99	0.466	0.63	0.702	1.05	0.433
Residual Error	16	-	-	-	-	-	-	-	-
Lack-of-Fit	10	1.43	0.344	0.97	0.542	1.51	0.317	1.11	0.471
Pure Error	6	-	-	-	-	-	-	-	-
Total	30	-	-	-	-	-	-	-	-

In this section, the combined effect of variation of two process parameters on each process response is analysed with surface plots obtained during MINITAB based data analysis. The influence of increase in laser beam average power and pulse frequency on surface roughness (Ra) in lateral direction is shown in figure 4, when laser beam scanning speed and transverse feed kept as constant at 3 mm/s and 0.03 mm, respectively. It is perceived from the surface plot that the surface roughness (lateral) values are increasing at all pulse frequency settings, with increase of laser beam average power. This is due to the fact that laser beam average power is directly proportional to the peak power of the beam which is also evident from the below mentioned equation.

$$\text{Peak power}\,(P_p)=\frac{\text{Average power}\,(P_A)}{\text{Pulse frequency}\,(F_p)\times\text{Pulse duration}\,(\mu)} \quad (7)$$

Thus, due to availability of sufficient energy in laser irradiated zone, the material melts and evaporates instantly which results in surface irregularities. In relation to Equation (1), for any

particular value of laser beam scanning speed, with the increase of pulse frequency the lateral overlap percentage increases. Thus, the value of surface roughness (lateral) further decreases due to the less height of micro-peaks generated on the machined surface. It is also depicted from the figure that, the surface roughness (lateral) values first increases and then decreases by increasing the pulse frequency. This is because of the fact that when pulse frequency is increasing, the laser beam interaction time with material surface is also increasing and thus, the crater size is also increasing. Consequently, the roughness values are increasing.

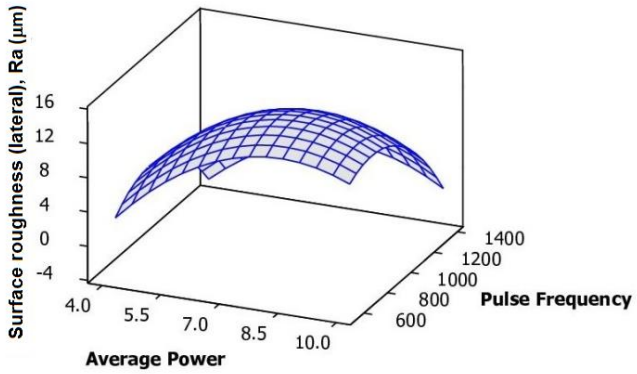

Figure 4. Effect of average power and pulse frequency on surface roughness (lateral), Ra

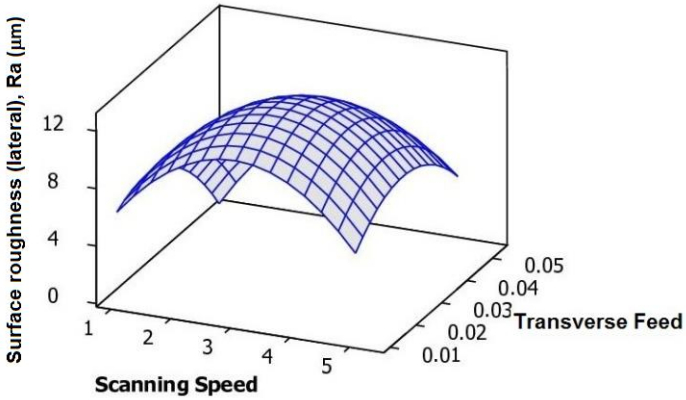

Figure 5. Effect of scanning speed and transverse feed on surface roughness (lateral), Ra

The effect of changing the laser beam scanning speed and transverse feed on surface roughness (lateral) values (Ra) when other process parameters were kept constant as average power at 7 W and pulse frequency at 1000 Hz as shown in figure 5. An increasing then decreasing trend of roughness value is observed from the figure by increasing the laser beam scanning speed. The roughness increases, due to the decreasing value of spot overlap, while increasing the scanning speed. Due to high scanning speed values, the interaction time decreases between laser beam and material which leads to less removal by laser irradiation and thus the surface has less irregularities. An increasing trend is observed for surface roughness from the figure while increasing the transverse feed. This phenomenon is also observed by the increase of transverse feed, where the values of transverse overlap between two laser scanning track decreases which results a lot of irregularities in the machined surface, ultimately leads to increase in the roughness.

The effect of variation of laser beam average power and pulse frequency on surface roughness (transverse), Ra is shown in figure 6, where process parameters like scanning speed and transverse feed are kept constant at a value 3mm/s and 0.03mm respectively. Due to the fact that as the average power is increasing the peak power is also increasing according to the relation (7), it can also be observed from the figure that surface roughness (transverse) shows an increasing trend with the increase of laser beam average power. Thus, due to availability of sufficient energy in laser irradiated

zone, the material melts and evaporates instantly which results in surface irregularities. As indicated in the the very same plot the surface roughness (transverse) decreases with the increase of pulse frequency. The equation (7) also explains this trend that shows with increasing pulse frequency the peak power will decrease, so the energy associated with the laser beam at the laser irradiated zone will also decrease and less amount of metal will be melted and vaporized from the zone. This result in formation of lower crater size with less irregularities and eventually surface roughness will decrease.

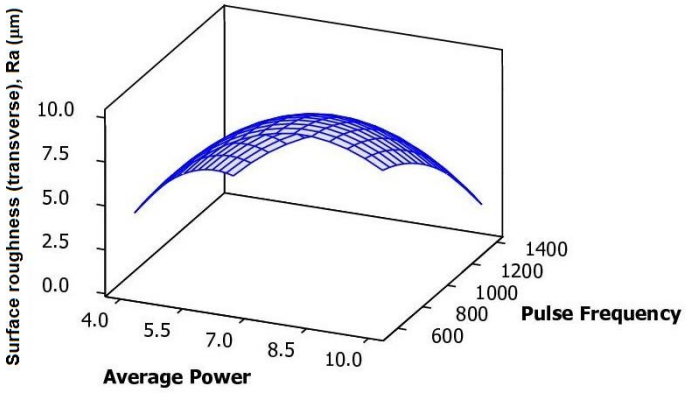

Figure 6. Effect of average power and pulse frequency on surface roughness (transverse), Ra

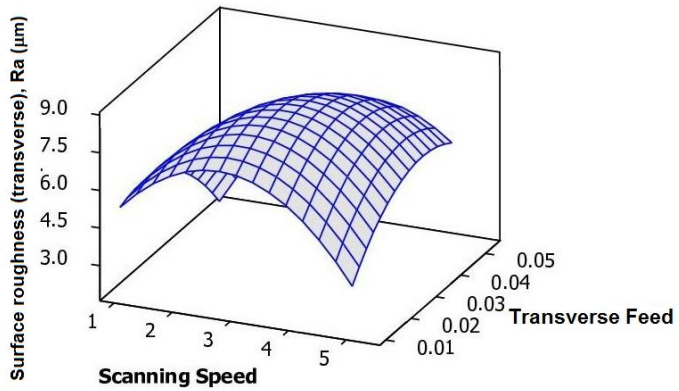

Figure 7. Effect of scanning speed and transverse feed on surface roughness (transverse), Ra

Variation of surface roughness (transverse), Ra with the variation of scanning speed and transverse speed is shown in figure 7, when the other two process parameter like laser beam average power and pulse frequency are kept constant at a value of 7 W and 1000 Hz. The figure shows the gradual increase and then steep decreasing characteristics of the surface roughness with the increase of scanning speed. This plot can be described as when the scanning speed increases with constant average power and transverse feed, the overlap distance between the two-consecutive laser scanning track decreases leading to decrease in surface roughness. This can also be derived from the same plot that the surface roughness (transverse) increases with the increase of transverse feed, which is evident from equation (2). As the transverse feed increases, the values of transverse overlap between two laser scanning track decreases eventually leads to lot of irregularities of the machined surface which ultimately increases the roughness.

Figure 8 shows the effect of variation of surface roughness (lateral), Rz on laser beam average power and pulse frequency keeping other two process parameters like scanning speed and transverse feed constant at a value of 3 mm/s and 0.03 mm respectively. The plot indicates the increase in surface roughness with the increase of laser beam average power. This is due to the increasing of peak power with the increase of laser beam average power according to equation (7). An increased peak power will generate more energy in the laser zone to melt and vaporize the metal, results in the production of

a deeper hole and further cause an increment in surface roughness. The same figure also depicts that the surface roughness (lateral) has a depreciating nature with the increase of pulse frequency. Increased pulse frequency leads to decrease in peak power that further causes decrement in surface roughness.

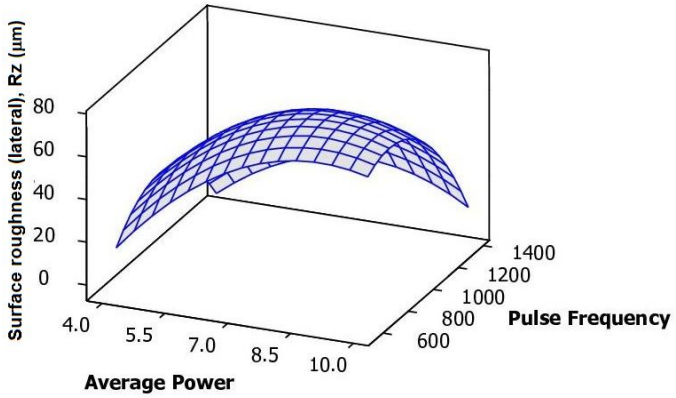

Figure 8. Effect of average power and pulse frequency on surface roughness (lateral), Rz

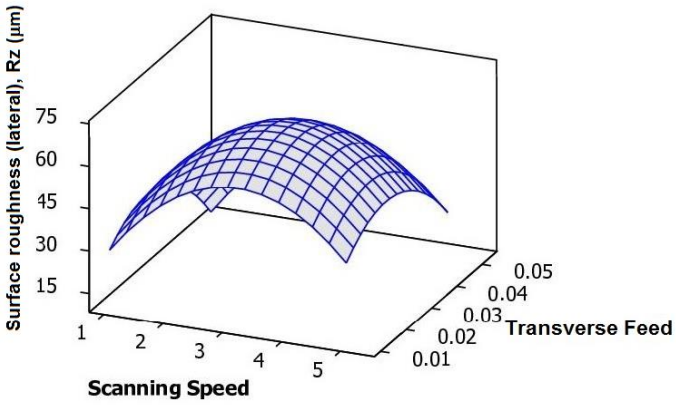

Figure 9. Effect of scanning speed and transverse speed on surface roughness (lateral), Rz

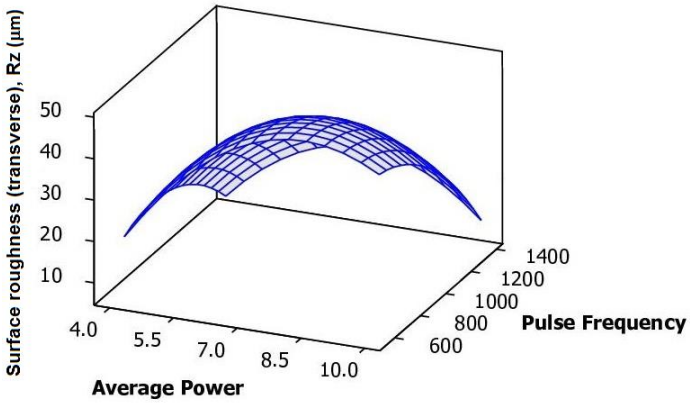

Figure 10. Effect of average power and pulse frequency on surface roughness (transverse), Rz

Figure 9 shows the effect of variation of surface roughness (lateral), Rz with the variation of scanning speed and transverse speed keeping the other two process parameter like laser beam average power and pulse frequency constant at a value of 7 W and 1000 Hz, respectively. The figure shows an increasing then followed by decreasing trend of the surface roughness curve with the increase of scanning speed, because of at lower scanning speed, the developed surface shows a decreased overlap between the two spots resulting in increased surface roughness. However, due to higher scanning

speed, the interaction time between the laser beam and the metal reduces considerably and it doesn't get ample time to melt and vaporize the metal as a result the surface roughness decreases. The very same plot indicates that with increase in surface roughness the transverse feed increases. This is due to the reason that, since with increase of transverse feed, the values of transverse overlap between two laser scanning track decreases and results in lot of irregularities of the machined surface which ultimately increases the roughness.

The effects of variation of surface roughness (transverse), Rz with the variation of laser beam average power and pulse frequency is shown in figure 10. Remaining two process parameters, scanning speed and transverse feed are kept at constant value of 3 mm/s and 0.03 mm, respectively. An increasing trend is observed for the surface roughness with increase in laser beam average power. Surface roughness increases due to the fact that an increase in laser beam average power causes an increment in peak power and that results in generation of more energy to melt and vaporize the metal. This figure also depicts that an inverse relation is observed between surface roughness and pulse frequency. Surface roughness is also observed to decrease, since the increase of pulse frequency decreases the peak power,

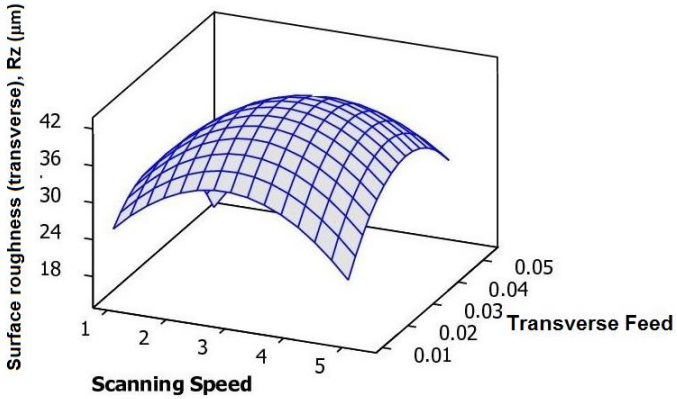

Figure 11. Effect of scanning speed and transverse feed on surface roughness (transverse), Rz

Figure 11 shows the effect of interaction of transverse surface roughness (Rz) with the variation of scanning speed and transverse speed keeping the other two process parameter, i.e., laser beam average power and pulse frequency constant at a value of 7 W and 1000 Hz, respectively. The figure shows a gradual increasing trend and then depreciating nature of the surface roughness curve with the increase of scanning speed. This is due to the reason that at lower scanning speed, the developed textured surface shows a decreased overlap between the two spots causing the surface roughness to increase. However, at the higher scanning speed, the interaction time between the laser beam and the metal reduces considerably without having ample time to melt and vaporize the metal thus results to decrease in surface roughness. It is depicted from the same figure that with increase in transverse feed, surface roughness increases. This is due the increase of transverse feed, the values of transverse overlap between two laser scanning track decreases and thus, the irregularities of the machined surface increases, which ultimately increases the roughness.

It is vital to consider optimization statistical tool to achieve multi objective optimization parametric combination of considered process parameters, to achieve minimum surface roughness values (Ra and Rz) simultaneously. The results of multi-objective optimization for achieving optimized values of process responses are shown in figure 12. The optimal process parameters obtained is with the combination of average power at 9.02 W, pulse frequency at 1340 KHz, laser beam scanning speed at 2.04mm/s and transverse feed at 0.0227mm. The optimal surface roughness (lateral), Ra obtained is 2.93 µm, surface roughness (transverse), Ra 3.32 µm, surface roughness (lateral), Rz 19.48 µm and surface roughness (transverse), Rz 18.89 µm. All the responses have been collected with composite desirability (D) value of 1, during multi objective optimization.

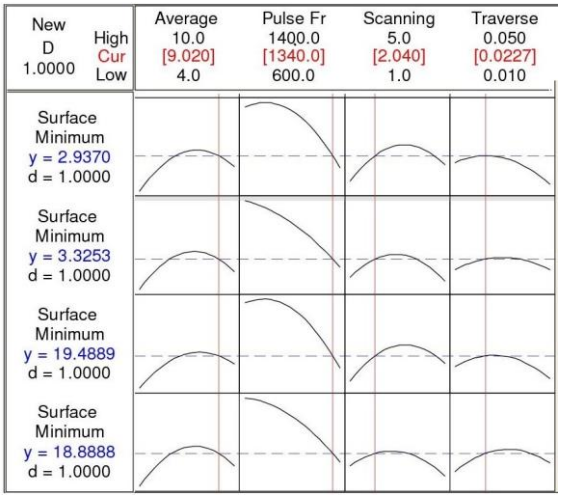

Figure 12. Results of Multi-objective optimization to obtain minimum surface roughness Ra and Rz

Verification and validation experiment of confirming the values of multi objective optimization was conducted at the nearer feasible parametric combination of multi objective optimized setting. Optimum values of surface roughness (lateral and transverse) were obtained as 3.01, 3.44 20.13 and 19.45 μm, respectively. As per the calculation, the values of prediction errors were 2.71, 3.43, 3.18 and 2.87%, very much within acceptable limit. Thus, the optimized parametric combination is valid within considered range of process parameters.

4. Conclusions

The present work deals with the experimental investigation and analysis of laser surface texturing process on titanium material using laser scanning strategy by pulsed Nd:YAG laser. RSM based experimental design was implemented to carryout experimental and further development of empirical models to correlate the process parameters and response criteria. The empirical models developed were validated through analysis of variance (ANOVA) test. it can be concluded that the process parameters such as laser beam average power, pulse frequency, scanning speed and transverse feed have significant influences to achieve quality surface. Multi-objective optimization parametric combination was also obtained for achieving least surface roughness (Ra and Rz) in lateral and transverse directions. Optimized response values were achieved as lateral surface roughness (Ra) of 2.93 μm, transverse surface roughness (Ra) of 3.32 μm, lateral surface roughness (Rz) of 19.48 μm and transverse surface roughness (Rz) of 18.89 μm at parametric combination of average power at 9 W, pulse frequency at 1400 Hz, laser beam scanning speed at 2 mm/s and transverse feed at 0.02 mm. this research will provide great impetus for effective and successful utilization of pulsed Nd:YAG laser during the tribological surface generation of specific surface properties for successful applications in the micro-parts manufacturing.

References

[1] Islam M U and Campbell G 1993 *Materials and Manufacturing Processes* **8** 611-630
[2] Roessler D M 1989 *Materials and Manufacturing Processes* **4** 285-310.
[3] Jackson M J, Whitfield M D, Robinson G M, Handy R G, Morrell J S, Ahmed W, Sein H 2015 Machining with Nanomaterials (Springer International Publishing Switzerland) p 77-127.
[4] Ali M Y, Hung W N P 2017 Comprehensive Materials Finishing vol 1 (Elsevier) p 322-343
[5] Meijer J 2004 *Journal of Materials Processing Technology* **149** 2–17
[6] Chang C W, Chen C Y, Chang T L, Ting C J, Wang C P, Chou C P 2012 *Applied Physics A* **109** 441–448
[7] Cunha A, Oliveira V, Vilar R 2016 Laser Surface Modification of Biomaterials: Techniques and Applications (Woodhead Publishing) p 301–322

[8] Dunn A, Wlodarczyk K L, Carstensen J V, Hansen E B, Gabzdyl J, Harrison P M, Shephard J D, Hand D P 2015 *Applied Surface Science Part B* **357** 2313-2319
[9] Toyserkani E, Rasti N 2014 Laser Surface Engineering (Woodhead Publishing) p 441-453
[10] Kovalchenko A, Ajayi O, Erdemir A, Fenske G, Etsion I 2004 *Tribology Transactions* **47** 299-307
[11] Li B J, Li H, Huang L J, Ren N F, Kong X 2016 *Applied Surface Science* **389** 585–593
[12] Soveja A, Cicala E, Grevey D, Jouvard J M 2008 *Optics and Lasers in Engineering* **46** 671–678
[13] Tripathi K, Joshi B, Gyawali G, Amanov A, Lee S W 2015 *Journal of Tribology* **138** 011601-011610
[14] Velasquez T, Han P, Cao J, Ehmann K F 2013 *Proceedings of the ASME 2013 International Manufacturing Science and Engineering Conference (Madison, Wisconsin, USA)* V001T01A009
[15] Vora H D, Dahotre N B 2015 *Journal of Manufacturing Processes* **19** 49–58